MAGMA EMPLACEMENT AND MANTLE SOURCE COMPOSITIONS INFERRED FROM A COMPREHENSIVE SUITE OF NAKHLITES AND CHASSIGNITES.

A. Udry[1], J. M. D. Day[2], and F. Moynier[3] [1]University of Nevada Las Vegas, Las Vegas NV 80154 (arya.udry@unlv.edu); [2]Scripps Institution of Oceanography, La Jolla, CA 92093; [3]Institut de Physique du Globe de Paris, 75005, Paris, France

Introduction: The cumulate martian nakhlites (clinopyroxenites) and chassignites (dunites), which now include 20 individually classified meteorites, likely originated from a similar magmatic system. This interpretation was based on their common crystallization (1.3 Ga) and ejection ages (11 Ma) [1], as well as their similar mineralogy and geochemistry [2,3]. However, these meteorites show variation in modal abundances in intercumulus material, as well as different cooling and equilibration histories. Numerous models have been proposed for the emplacement of nakhlites and chassignites, including one to several lava flows or formation in a shallow sill [e.g., 3-9]. Given these relationships, nakhlites and chassignites have the potential to be studied as a cogent suite of samples to establish parental melt compositions and possible emplacement mechanisms. However, no study has been done to examine these meteorites as a suite. Here we present a coherent study of nakhlites and chassignites, including bulk-rock chemical (13 nakhlites and 2 chassignites) and textural (8 nakhlites) analyses, including Crystal Size Distribution (CSD) and Spatial Distribution Patterns (SDP) analyses. We also present data from the newly classified nakhlite Northwest Africa (NWA) 11013.

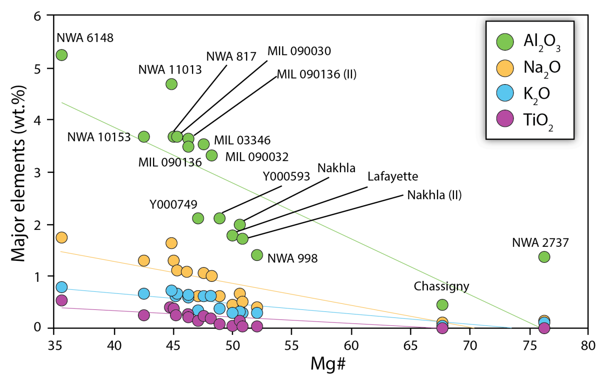

Figure 1. Major element concentrations (Al_2O_3, Na_2O, K_2O, TiO_2 in wt.%) in nakhlites and chassignites (some include duplicates) and regression lines for each oxide.

Methods: Bulk-rock major and trace element concentrations were obtained at *the Scripps Isotope Geochemistry Laboratory* using a *ThermoScientific* iCAP Qc quadrupole ICP-MS in normal mode. Analyses were standardized versus reference material BHVO-2. In addition, reference materials were analyzed as "unknowns" (AGV-1, BHVO-2, and BCR-2) to assess external reproducibility and accuracy. For major and trace elements, reproducibility of the reference materials was generally better than 6% (RSD), except for Se, Sn and Mo (<12% RSD).

For CSD and SDP analyses, pyroxene and olivine grain boundaries were traced using transmitted and reflected light image mosaics and converted to length and width measurements using the software *ImageJ*. Measurements were inputted into CSD*slice* software [10] for a true three-dimensional crystal size distribution. Best matching habit ratios (long-, intermediate-, and short-axis ratio) were calculated with CSD*slice* and entered in the CSD*corrections* software [11] to generate the CSD plots (Fig. 1). The R-value was obtained using Big-R available in CSD*corrections* for the pyroxene population [12]. Modal abundances were measured using pixel count in *ImageJ.*

Bulk-rock major and trace element analyses: The fifteen analyzed nakhlites and chassignites have MgO ranging from 7.3 to 35.8 wt.% (up to 12.3 wt.% for nakhlites, exclusively) and Mg#s from 35.6 to 76.2 (Fig. 1). These ranges are similar to cumulate basaltic intrusions on Earth. The abundances of major and trace incompatible elements increase with decreasing Mg# and with increase in intercumulus material abundance. A 1.5 wt.% gap in Al_2O_3 is observed between the paired Yamato nakhlites (Y000593 and Y000749) and NWA 817 nakhlites. The increase in TiO_2 with increasing intercumulus material is likely consistent with increase in titanomagnetite abundance (Fig. 1). In addition, the newly classified NWA 11013 shows a MgO content similar to NWA 10153, the Miller Range nakhlites, and NWA 817; however, it displays the lowest FeO content relative to the other nakhlites (16.7 wt.%). The abundances of compatible elements (Ni, Cr, Co, and Ga) systematically increase with increasing MgO content as expected for cumulate rocks. All the samples show light rare earth elements (LREE) enrichments with small $[La/Yb]_{CI}$ variations between 3.2 and 5.9 that do not correlate with Mg#. The overall enrichment in trace elements is consistent with increasing intercumulus material. We observe overall negative anomalies in Zr and Hf for all the nakhlites and chassignites, which could be explained by residual garnet in the source, as seen in terrestrial komatiites [13; 14], as also shown by depletion of Y and heavy REE, and low U/Th. This reinforces the concept that nakhlites and chassignites originated from the same source. Large Ba positive anomalies and high Ba/Rb are observed in the NWA nakhlites, indicating hot desert terrestrial contamination.

Textural analyses: Modal abundances of the eight measured nakhlites are within error of the different nakhlite thin sections from previous studies [5].

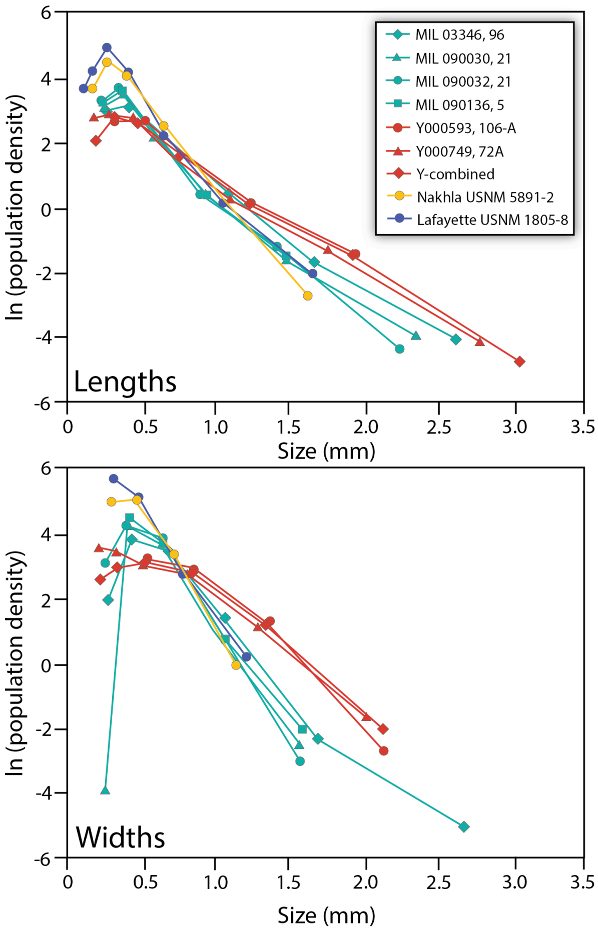

Figure 2. CSD plots (population density versus size in mm) of pyroxene population (lengths and widths) of the Miller Range nakhlite, Yamatos, Lafayette, and Nakhla.

Crystal Size distribution. The CSD analyses are presented in Fig 2. The CSD slopes go from shallow to steep in the following order: Yamatos - Miller Range - Nakhla - Lafayette. The paired meteorites (Miller Range and Yamato nakhlites) show similar slopes and modal abundances within error. In a single lava flow, we would expect the samples located closer to the bottom (Lafayette) to show the longest magma residence time (steepest slope) with CSD slopes representing textural coarsening. However, the fact that the Yamatos show the longest residence time might confirm the crystal mush model of [5] or might indicate a different magma pulse. In addition, the Yamatos shallow slopes might be due to the fact that the studied samples show less pyroxene grains (<250 grains) than needed for CSD analyses [11]. Using CSD plot slopes and growth rates of 10^{-9} mm/s and [15,16] and 10^{-10} mm/s [17], we estimate residence times between 5 and 111 years.

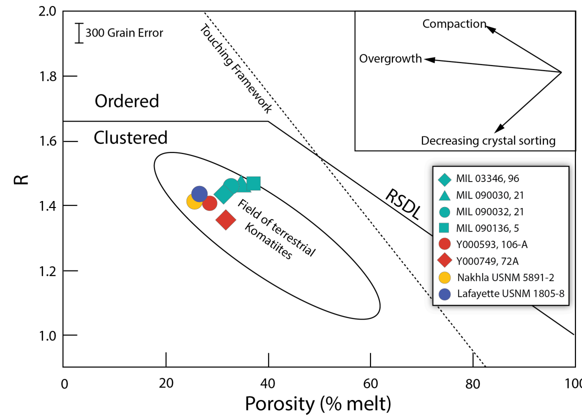

Figure 3. SDP analyses for same meteorites as figure 2. R is defined as the ratio of the mean nearest neighbor distance of the phase to the predicted mean nearest neighbor distance for a random distribution of points.

Spatial Distribution patterns. The SDP analyses show that the nakhlites all fall within "clustered" touching framework field, indicating that the pyroxene grains formed as clumps during accumulation. In this manner, they form similarly to terrestrial komatiite flows (Fig. 3). The nakhlites show a slight decrease in R-value with decreasing porosity (corresponding to the melt %), which could represent decreasing crystal sorting. However, more samples are needed to make any conclusions on SDP.

Acknowledgements: We thank Tim McCoy (Smithsonian Institution), the Japanese Antarctica collection, the JSC MWG, and Luc Labenne and Mendy Ouzillou for providing the samples.

References: [1] Nyquist (2001) *JGR 90,* 1151–1154. [2] McCubbin F. M. et al. (2013) *Meteoritics & Planet. Sci 48*, 819-853. [3] Day J. M. D. (2006) *Meteoritics & Planet. Sci. 41,* 581-606. [4] Udry A. et al. (2012) *Meteoritics & Planet. Sci. 47*, 1575-1589. [5] Corrigan C.M. (2015) *Meteoritics & Planet. Sci. 50*, 1497-1511 [6] Treiman A [7] Jambon A. et al. (2016) *GCA 190,* 191-212. [8] Richter F. et al. (2016) *GCA 182*, 1-23 [9] Balta J. B. et al. (2016) *Meteoritics & Planet. Sci. 1-24.* [10] Morgan D. J. and Jerram D. A. (2006) *Jour. Volc. Geoth. Res. 154*, 1–7. [11] Higgins M. D. (2000) *Am. Min. 85*, 1105-1116. [12] Jerram D.A. (1996) *Contr. Min. Petr. 125,* 60-74. [13] Xie Q. et al. (1993) *GCA 57*, 4111–4118. [14] Polat A. et al. (1999) *Precamb. Res. 94,* 139-173. [15] Cashman and Marsh (1988) *Contr. Min. Petr. 99,* 292-305; [16] Jerram et al. (2003) *J. Petrol. 44*, 2033-2051; [17] Leu et al. (2010) *GSA* 42, 100.